# Effects of a Toroidal Rotation on the Stability Boundary of the MHD Modes in the Tokamak Edge Pedestal

N. Aiba 1), S. Tokuda 1), M. Furukawa 2), N. Oyama 1) and T. Ozeki 1)

1) Japan Atomic Energy Agency, Naka, Ibaraki 311-0193, Japan
2) Graduate School of Frontier Science, University of Tokyo, Kashiwa, Chiba 277-8561, Japan

e-mail contact of main author: aiba.nobuyuki@jaea.go.jp

**Abstract.** Effects of a toroidal rotation are investigated numerically on the stability of the MHD modes in the edge pedestal, which relate to the type-I edge-localized mode (ELM). A new linear MHD stability code MINERVA is developed for solving the Frieman-Rotenberg equation, which is the linear ideal MHD equation with flow. As the result of the stability analysis, it is revealed that the sheared toroidal rotation destabilizes the edge localized MHD modes. The change of the safety factor profile affects this destabilizing effect. This is because the rotation effect on the edge MHD stability becomes stronger as the toroidal mode number of the unstable MHD mode increases, and this toroidal mode number strongly depends on the safety factor profile.

## 1. Introduction

An ideal magnetohydrodynamic (MHD) mode unstable near the plasma surface is the cause of the type-I edge-localized mode (ELM), which constrains the maximum pressure gradient in the pedestal at the tokamak edge region. From the viewpoint of the heat load on the divertor, the type-I ELM needs to be suppressed or its amplitude needs to be reduced. The recent experimental results in JT-60U show that the toroidal rotation near the pedestal has an impact on the ELM phenomena. For example, in JT-60U, the ELM frequency changes from $\sim$ 20Hz to $\sim$ 1.4kHz as the toroidal rotation frequency decreases from 1kHz to $-$3kHz[1], where the sign of the rotation frequency is determined by the direction relative to the plasma current. In other words, the type-I ELM changes to the grassy-ELM as the toroidal rotation decreases. Such a change of the ELM frequency is observed only in a high-$q$, high-$\beta_p$, and strongly shaped equilibrium, where $q$ is the safety factor, $\beta_p$ is the poloidal beta value. Since the previous work showed that the cause of the grassy-ELM is also the ideal MHD mode whose mode structure is narrower than that of the type-I ELM[2], it is necessary to understand the toroidal rotation effects on the edge MHD stability analytically and numerically. As one of the past numerical studies, in Ref.[3], the authors investigated the dependence of the growth rate on the rotational shear in several $n$ cases, and illustrated that the rotational shear destabilizes the low-$n$ MHD mode but stabilizes the high-$n$ MHD mode. However, it is also important to understand the toroidal rotation effect on the stability boundary of the edge localized MHD modes.

In this paper, we focus on the toroidal rotation effect on the stability boundary of the edge localized MHD mode. As is well known, since the plasma rotation violates the Hermitian property of the linear ideal MHD equation[4], the eigenvalue problem approach with the normal mode analysis is sometimes inadequate to solve such a non-Hermitian problem; this is because a set of the particular solutions with variable separation is not generally complete unlike in a hermitian system. For solving numerically such a non-Hermitian problem with high accuracy, we develop a new linear MHD stability code MINERVA (Mhd INitial value and Eigenvalue pRoblems solver with a VAriational principle) that solves the linear ideal MHD equation with a toroidal rotation as the initial value problem[5]. With this code and the MHD spectrum code MARG2D[6, 7], we investigate the effect of a toroidal rotation on the stability boundary of edge localized MHD mode. Particularly, we pay attention to the difference between the rotation effects in the low-$q$ and high-$q$ equilibria.

This paper is organized as follows. Section 2 introduces the basic equations of the MINERVA code for the stability analysis of ideal MHD modes in a rotating axisymmetric equilibrium. Section 3 describes the results of stability analysis of edge localized MHD modes in the low-$q$ and the high-$q$ equilibria. Section 4 presents a summary of this work.

## 2. Basic Equations

To investigate the rotation effect on the macroscopic phenomena in tokamaks, we adopt the single-fluid ideal magnetohydrodynamic (MHD) equations with flow. In this paper, we consider an equilibrium rotation in the toroidal direction as

$$\boldsymbol{u}_0 = R^2\Omega(\psi)\nabla\phi, \tag{1}$$

where $\boldsymbol{u}_0$ is the equilibrium velocity, $\Omega(\psi)$ is the rotation frequency and $\psi(R,Z)$ is the poloidal flux function in the cylindrical coordinate system $(R,Z,\phi)$. As mentioned in Ref.[8], the equilibrium can be obtained by solving the Grad-Shafranov equation with toroidal flow

$$\Delta^*\psi = -R^2\left.\frac{\partial p}{\partial\psi}\right|_R - F(\psi)\frac{dF(\psi)}{d\psi}, \tag{2}$$

$$\Delta^* \equiv \frac{\partial^2}{\partial R^2} - \frac{1}{R}\frac{\partial}{\partial R} + \frac{\partial^2}{\partial Z^2}, \tag{3}$$

where $p$ is the plasma pressure and $F$ is the toroidal magnetic field function. With the isothermal condition on each magnetic surface $T = T(\psi)$, $p$ can be written as

$$p = p_0(\psi)\exp\left[M^2\left(\frac{R^2}{R_0^2} - 1\right)\right], \tag{4}$$

where $T$ is the ion temperature and $M$ is the Mach number defined as a ratio of the toroidal rotation velocity $v_\phi = R_0\Omega$ to the ion thermal velocity $v_{th} = \sqrt{2T/m_i}$,

$$M^2(\psi) \equiv \left(\frac{v_\phi}{v_{th}}\right)^2 = \frac{m_i R_0^2\Omega^2}{2T} = \frac{\rho R_0^2\Omega^2}{2p}. \tag{5}$$

The linear MHD stability in the equilibrium with flow can be identified by solving the Frieman-Rotenberg equation[9]

$$\rho\frac{\partial^2\boldsymbol{\xi}}{\partial t^2} + 2\rho(\boldsymbol{u}_0\cdot\nabla)\frac{\partial\boldsymbol{\xi}}{\partial t} = \boldsymbol{F}(\boldsymbol{\xi}), \tag{6}$$

$$\boldsymbol{F} = \boldsymbol{F}_s + \nabla\cdot\left[\rho\boldsymbol{\xi}(\boldsymbol{u}_0\cdot\nabla)\boldsymbol{u}_0 - \rho\boldsymbol{u}_0(\boldsymbol{u}_0\cdot\nabla)\boldsymbol{\xi}\right], \tag{7}$$

$$\boldsymbol{F}_s = \nabla\left[\boldsymbol{\xi}\cdot\nabla p + \Gamma p\nabla\cdot\boldsymbol{\xi}\right] + (\nabla\times\boldsymbol{Q})\times\boldsymbol{B} + \boldsymbol{j}\times\boldsymbol{Q}. \tag{8}$$

Here $\boldsymbol{\xi}$ is the Lagrangian displacement, $\rho$ is the plasma density, $\boldsymbol{F}_s$ is the static part of the force operator, $\Gamma$ is the ratio of the specific heats, $\boldsymbol{j}$ is the plasma current density, and $\boldsymbol{Q}$ is the fluctuation of the magnetic field given by

$$\boldsymbol{Q} \equiv \nabla\times(\boldsymbol{\xi}\times\boldsymbol{B}). \tag{9}$$

As already mentioned in Ref.[4], in the bilinear form (weak form) of Eq.(6) obtained by introducing the vector function $\boldsymbol{\eta}$, the force operator term

$$W_p[\boldsymbol{\eta},\boldsymbol{\xi}] = -\int\boldsymbol{\eta}^*\cdot\boldsymbol{F}(\boldsymbol{\xi})d\tau = \left\langle\boldsymbol{\eta}\left|\mathbf{W}_p\right|\boldsymbol{\xi}\right\rangle, \tag{10}$$

and the kinetic energy term

$$K[\boldsymbol{\eta},\boldsymbol{\xi}] = \int \boldsymbol{\eta}^* \cdot \rho \frac{\partial^2 \boldsymbol{\xi}}{\partial t^2} d\tau = \left\langle \boldsymbol{\eta} \middle| \mathbf{K} \middle| \frac{\partial^2 \boldsymbol{\xi}}{\partial t^2} \right\rangle, \tag{11}$$

retain a hermitian property as those in the static case[10], but the convective term

$$U[\boldsymbol{\eta},\boldsymbol{\xi}] = \int \boldsymbol{\eta}^* \cdot \rho(\boldsymbol{u}\cdot\nabla)\boldsymbol{\xi} d\tau = \left\langle \boldsymbol{\eta} \middle| \mathbf{U} \middle| \frac{\partial \boldsymbol{\xi}}{\partial t} \right\rangle, \tag{12}$$

has an anti-hermitian property $U[\boldsymbol{\eta},\boldsymbol{\xi}] = -U^*[\boldsymbol{\xi},\boldsymbol{\eta}]$. Due to this anti-hermitian convective term, an ideal MHD stability problem with an equilibrium flow becomes a non-hermitian problem, unlike that in a static system (Energy Principle).

Moreover, to investigate the stability of external (free boundary) MHD modes, we need to calculate the potential energy of the vacuum magnetic field surrounding the plasma, $\mathcal{W}_V$. The MARG2D code adopts a useful numerical method for estimating $\mathcal{W}_V$ with the vector potential technique, and realizes to investigate the stability of a wide $n$ range of external MHD modes in a static equilibrium with a high level of accuracy[11]. With this technique, the perturbed magnetic fields in the vacuum $\boldsymbol{Q}_V$ are expressed as

$$\boldsymbol{Q}_V = \nabla \times \boldsymbol{A}, \quad \boldsymbol{A} \equiv \boldsymbol{\xi}_V \times \boldsymbol{C}_V, \tag{13}$$

where $\boldsymbol{\xi}_V$ is the unknown vector called a pseudo-displacement vector in the vacuum, $\boldsymbol{C}_V$ is the solenoidal field ($\nabla \cdot \boldsymbol{C}_V = 0$) defined as

$$\boldsymbol{C}_V = \nabla\phi \times \nabla\psi_V + T_V \nabla\phi, \tag{14}$$

$\psi_V$ is the quasi-magnetic surfaces in the vacuum, and $T_V$ is a function of $\psi_V$ and $\zeta$ in the auxiliary coordinate system $(\rho, \zeta, \phi)$

$$R = R_0 + \rho\cos\zeta, \quad Z = \rho\sin\zeta, \tag{15}$$

where $R_0$ is the major radius of the plasma. With this $\boldsymbol{\xi}_V$ and the vector function $\boldsymbol{\eta}_V$, $\mathcal{W}_V$ can be expressed as

$$\mathcal{W}_V = 2\pi^2 \int_{\psi_p}^{\psi_{Vmax}} \left\langle \boldsymbol{\eta}_V \middle| \mathbf{W}_V \middle| \boldsymbol{\xi}_V \right\rangle d\psi_V, \tag{16}$$

where the continuous condition of the normal component of the perturbed magnetic field $\boldsymbol{Q}\cdot\boldsymbol{n}$ at the plasma surface ($r = a_0$, $\psi_V = \psi_p$) is given as

$$\boldsymbol{\xi}\cdot\nabla\psi|_{r=a_0} = \boldsymbol{\xi}_V \cdot \nabla\psi_V|_{\psi_V=\psi_p} = Y_V(\psi_V = \psi_p), \tag{17}$$

$a_0$ is the plasma minor radius, and $\psi_{Vmax}$ is the $\psi_V$ value at the wall, which can be determined arbitrary. Since this bilinear form does not change in the case including a toroidal rotation, we obtain the bilinear form including the vacuum energy as

$$\int_0^{a_0} \left[ \left\langle \boldsymbol{\eta} \middle| \mathbf{K} \middle| \frac{\partial^2 \boldsymbol{\xi}}{\partial t^2} \right\rangle + 2\left\langle \boldsymbol{\eta} \middle| \mathbf{U} \middle| \frac{\partial \boldsymbol{\xi}}{\partial t} \right\rangle + \left\langle \boldsymbol{\eta} \middle| \mathbf{W}_{ps} - \mathbf{W}_{pd} \middle| \boldsymbol{\xi} \right\rangle \right] dr + \int_{\psi_p}^{\psi_{Vmax}} \left\langle \boldsymbol{\eta}_V \middle| \mathbf{W}_V \middle| \boldsymbol{\xi}_V \right\rangle d\psi_V = 0. \tag{18}$$

On the basis of this bilinear form Eq.(18), we have developed the MINERVA code with the finite element method (FEM). Since the normal mode approach ($\boldsymbol{\xi} \propto \exp(\iota\omega t)$) is not necessarily suitable for capturing the fastest growing instability in a non-hermitian system, the MINERVA code solves not only the eigenvalue problem but also the initial value problem[5].

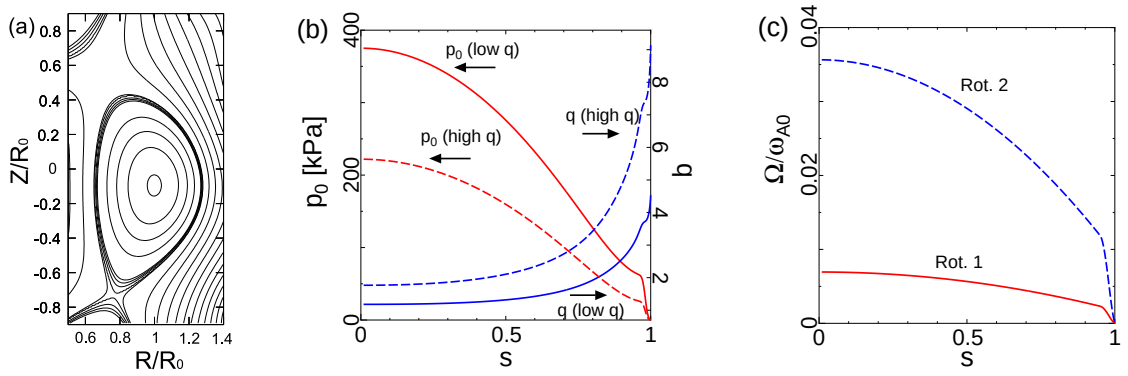


*FIG. 1. (a) Contours of the poloidal magnetic flux $\psi$ (magnetic surfaces) of the ITER-like D-shape equilibrium. (b) Profiles of $p_0$ (red line) and $q$ (blue line) in the low-$q$ equilibrium (solid line) with $C_p = 4.00$ and $C_j = 0.60$ and the high-$q$ equilibrium (broken line) with $C_p = 2.60$ and $C_j = 0.65$, respectively. (c) Profiles of the toroidal rotation frequency of the profiles Rot.1 and Rot.2 normalized with the toroidal Alfvén frequency at the axis $\omega_{A0}$.*

## 3. Effect of the toroidal rotation on the edge MHD stability

In this section, we investigate an effect of the toroidal rotation on the stability of edge localized MHD modes with the MINERVA code. As mentioned in Introduction, we pay attention to the difference between the rotation effects in the low-$q$ and high-$q$ equilibria.

The equilibrium analyzed in this paper has a ITER-like D-shape cross-section that will be realized in JT-60SA future device; the ellipticity $\kappa$ and triangularity $\delta$ are $(1.65, 0.35)$ in the upper side and $(2.00, 0.58)$ in the downer side as shown in Fig.1(a). The parameters ($R_0$[m], $a_0$[m], $B_{t0}$[T]) are (3.00, 0.97, 4.00), and the profiles of $dp_0/d\psi$ and $\langle \boldsymbol{j}\cdot\boldsymbol{B}\rangle/\langle B^2\rangle$ are given as

$$\frac{dp_0(\psi)}{d\psi} = \beta_p \left( \left(1.00 - \psi^{5.0}\right)^{1.5} + C_p \cdot \exp\left(\frac{(\psi - 0.96)^2}{2.25\times 10^{-4}}\right)\right), \tag{19}$$

$$\frac{\langle \boldsymbol{j}\cdot\boldsymbol{B}\rangle}{\langle B^2\rangle} \propto \left(1.0 - \psi^{1.5}\right)^{1.2} + 0.15\exp\left(\frac{(\psi - 0.91)^2}{1.44\times 10^{-2}}\right)\cdot\cos\left(\frac{\pi}{2}\psi^{10}\right) + C_j \cdot \exp\left(\frac{(\psi - 0.96)^2}{4.00\times 10^{-4}}\right), \tag{20}$$

where $a_0$ is the minor radius of the plasma and $B_{t0}$ is the toroidal magnetic field at the axis. The second term in RHS of Eq.(19) and the third term in RHS of Eq.(20) make the steep pressure gradient and the virtual edge bootstrap current density near $\psi = 0.96$, respectively. Hereafter, $\psi$ is normalized as $\psi = 0$ at the axis and $= 1$ at the plasma surface. The plasma current $I_p$ and the poloidal beta value $\beta_p$ are determined as $(I_p[\mathrm{MA}], \beta_p) = (4.90, 0.64)$ in the low-$q$ equilibria and $(2.60, 1.20)$ in the high-$q$ equilibria; the normalized beta values $\beta_N$ are almost same as 2.00. The typical profiles of $p_0$ and $q$ in the low-$q$ equilibrium with $C_p = 4.00$ and $C_j = 0.65$ and those in the high-$q$ equilibrium with $C_p = 2.60$ and $C_j = 0.60$ are shown in Fig.1(b). We investigate the stability boundary of the edge localized MHD modes in these equilibria by changing the parameters $C_p$ and $C_j$.

The equilibrium rotation profile is determined as

$$\Omega(\psi)[\mathrm{kHz}] = \begin{cases} \Omega_{0m} + (\Omega_{0i} - \Omega_{0m})\cdot\left(1.00 - \left(\frac{\psi}{0.90}\right)\right) & (\psi \le 0.90), \\ g_1 - g_2 + (\Omega_{0m} + g_2)\cdot\left(1.00 - \left(\frac{\psi - 0.90}{0.10}\right)^2\right)^2 & (\psi > 0.90), \end{cases} \tag{21}$$

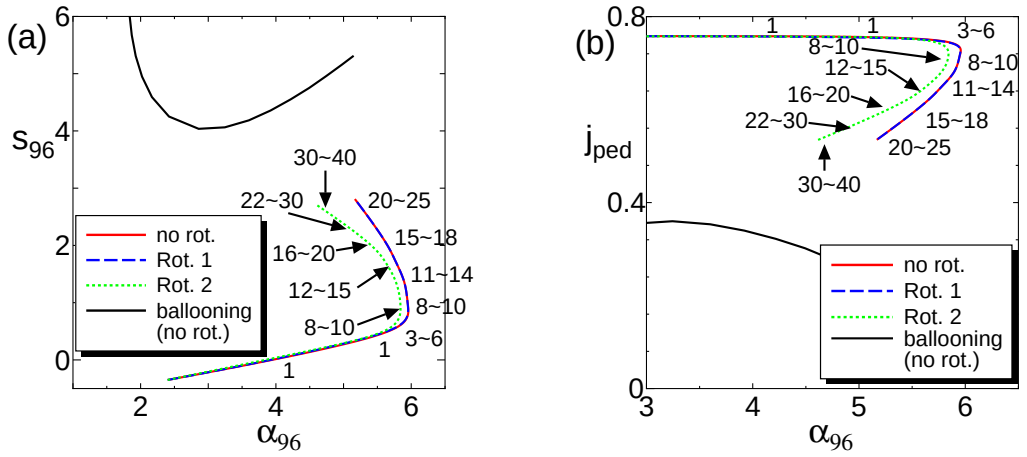


*FIG. 2. Stability diagram of the low-q equilibria on (a) the $s_{96}$-$\alpha_{96}$ plane and (b) the $j_{ped}$-$\alpha_{96}$ plane in each rotation profile (no rotation, Rot.1, and Rot.2) case. The numbers in these figures show the n number of the most unstable MHD mode at each ($s_{96}$, $\alpha_{96}$)/($j_{ped}$, $\alpha_{96}$). The edge localized MHD modes become unstable as the sheared rotation increases, and this destabilizing effect of the sheared rotation becomes stronger as the n number of the MHD mode increases.*

where $\Omega_{0i}$ and $\Omega_{0m}$ are the rotation frequencies at $\psi = 0.00$ and 0.90, and

$$g_1 = (\Omega_{0i} - \Omega_{0m}) \cdot \left(1.00 - \left(\frac{\psi}{0.90}\right)\right), \tag{22}$$

$$g_2 = (\Omega_{0i} - \Omega_{0m}) \cdot \left(1.00 - \left(\frac{1.00}{0.90}\right)\right) \simeq -0.11 \cdot (\Omega_{0i} - \Omega_{0m}). \tag{23}$$

We investigate an effect of the toroidal rotation on the edge MHD stability by changing ($\Omega_{0i}$[kHz], $\Omega_{0m}$[kHz]) from (0.00, 0.00) to (9.00, 3.00), named Rot.1, and (45.00, 15.00), named Rot.2; the profile Rot.1 is similar to the experimental data in JT-60U E46109[1] and the profile Rot.2 is five times larger than the profile Rot.1. These $\Omega(\psi)/\omega_{A0}$ profiles are shown in Fig.1(c), where $\omega_{A0}$ is the toroidal Alfvén frequency at the axis. The density profile in each equilibrium is assumed as constant. The $n$ range of the MHD mode analyzed numerically is from 1 to 40, and the mesh number $NR$ and the minimum/maximum truncated poloidal mode numbers $M_{min}/M_{max}$ are determined to obtain the well-converged growth rate in each $n$ case. The conducting wall surrounding the plasma is placed at $d/a = 2.00$, where $d$ is the minor radius of the conducting wall.

### 3.1. Rotation Effect in the low-$q$ equilibrium

In this subsection, we investigate a rotation effect on the stability of edge localized MHD modes in the low-$q$ equilibrium. Figure 2 shows the results of the stability analysis in the low-$q$ equilibria on (a) the $s_{96}$-$\alpha_{96}$ plane and (b) the $j_{ped}$-$\alpha_{96}$ plane, where $s$ is the magnetic shear defined as $s \equiv 2V/q(dq/dV)$, $V$ is the volume, $\alpha$ is the normalized pressure gradient as $\alpha \equiv -(\mu_0/2\pi^2)(dp/d\psi)(dV/d\psi)(VR/2\pi)^{0.5}$, $\mu_0$ is the permeability in the vacuum, the subscript 96 expresses the value at $\psi = 0.96$, and $j_{ped}$ is the volume averaged current density near the pedestal ($0.92 < s < 1.00$) normalized with the volume averaged current density in the plasma. As shown in these figures, the stability boundary of edge localized MHD modes in the rotating equilibrium with profile Rot.1 is almost same as that in the static equilibrium, but that in the rotating equilibrium with profile Rot.2 moves to the smaller $\alpha_{96}$ side. As the result of such a shift of the stability boundary, the maximum pressure gradient becomes smaller from

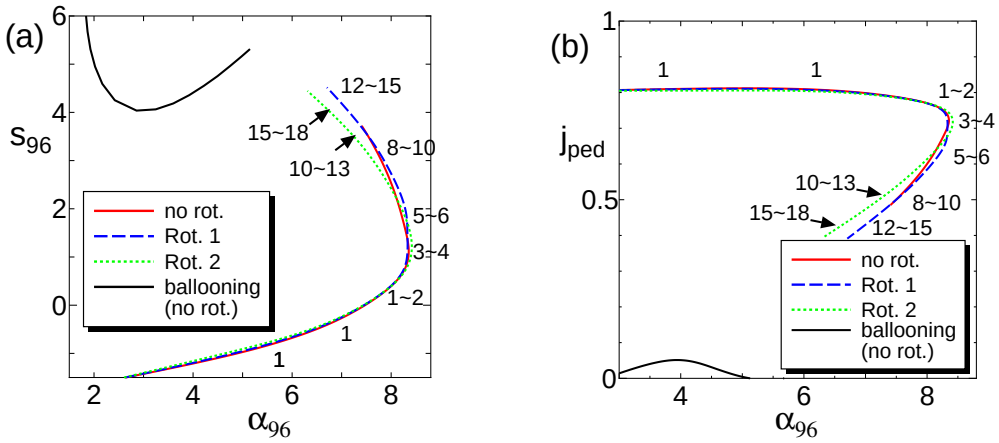


*FIG. 3. Stability diagram of the high-q equilibria on (a) the $s_{96}$-$\alpha_{96}$ plane and (b) the $j_{ped}$-$\alpha_{96}$ plane in each rotation profile (no rotation, Rot.1, and Rot.2) case. The numbers in these figures show the n number of the most unstable MHD mode at each ($s_{96}$, $\alpha_{96}$) / ($j_{ped}$, $\alpha_{96}$). The edge localized MHD modes become unstable as the sheared rotation increases, but the effect of the sheared rotation on the stability boundary is weaker than that in the low-q equilibria shown in Fig.2.*

$\alpha_{96-max} \simeq 5.99$ to $\simeq 5.85$ as the rotation increases. Moreover, the $n$ number of the MHD modes, which determine the stability boundary, becomes larger as the rotation frequency increases, and the destabilizing effect of the sheared toroidal rotation becomes stronger as the $n$ number of the MHD mode increases. This result is consistent with the results of the qualitative and quantitative analyses of the rotation and the rotational shear effects on the edge MHD stability in Ref.[5], and the main reason of this destabilization is thought as the rotational shear near the plasma surface.

### 3.2. Rotation Effect in the high-$q$ equilibrium

Next, in this subsection, we investigate the rotation effect on the edge MHD stability in the high-$q$ equilibrium. Figure 3 shows the stability diagrams in the high-$q$ equilibria on (a) the $s_{96}$-$\alpha_{96}$ plane and (b) the $j_{edge}$-$\alpha_{96}$ plane. As in the low-$q$ case shown in Fig.2, the stability boundary in the rotating equilibrium with profile Rot.1 is almost same as that in the static equilibrium, and that in the rotating equilibrium with profile Rot.2 also moves to the smaller $\alpha_{96}$ side. However, there are three differences between the results in the low-$q$ and the high-$q$ cases. One is the maximum pressure gradient at $\psi = 0.96$; in the high-$q$ case, $\alpha_{96}$ can reach to 8.41 though the maximum $\alpha_{96}$ is restricted near 5.99 in the low-$q$ static case. The second is the destabilizing effect of the toroidal rotation. In the high-$q$ case, since this destabilizing effect is weaker than that in the low-$q$ case, the maximum pressure gradient at $\psi = 0.96$ is almost unchanged though the rotation profile becomes Rot.2. The last one is the $n$ numbers of the edge localized MHD modes that determine the stability boundary. In the high-$q$ equilibria, the $n$ numbers of the MHD modes are smaller than those in the low-$q$ equilibria; for example, the $n$ number of the MHD mode that restricts the maximum pressure gradient changes from 9 in the low-$q$ case to 4 in the high-$q$ case.

The reason of these differences is thought as the difference of the infinite-$n$ ballooning mode stability near the pedestal. Figure 4 shows the stability diagram of the edge localized MHD modes and the infinite-$n$ ballooning mode on the $s$-$\alpha$ plane at $\psi = 0.96$, 0.97, and 0.98 in (a) the low-$q$ and (b) the high-$q$ static equilibria, respectively. As shown in these figures, the second stability region of ballooning mode in the high-$q$ equilibria is wider than that in the low-$q$ ones at

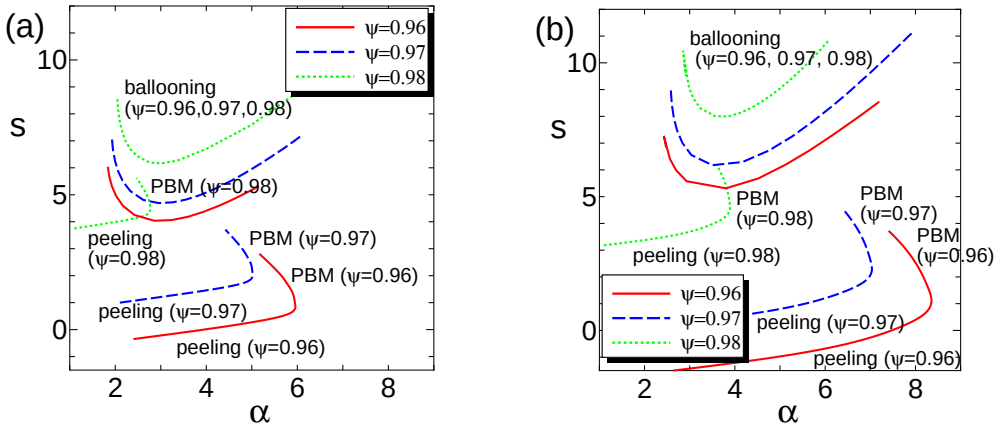


*FIG. 4. Stability diagram of the edge localized MHD modes and the infinite-n ballooning mode on the s-α plane at ψ = 0.96, 0.97, and 0.98 in (a) the low-q and (b) the high-q equilibria. The notes in these figures show the kind of the MHD modes, the kink/peeling mode, the ballooning mode, and the peeling-ballooning mode (PBM), that restrict the stability boundary at each (s, α) point. The second stability region of ballooning mode in the high-q equilibria is wider than that in the low-q equilibria; particularly, the minimum s of the ballooning mode stability boundary at ψ = 0.98 increases from s 6.20 to 8.00.*

each magnetic surface; particularly, at $\psi = 0.98$, the minimum $s$ of the ballooning mode stability boundary increases from $s \sim 6.20$ to $\sim 8.00$. In general, the stability boundary of current-driven kink/peeling mode, which is the lower stability boundary of $s$, is mainly determined by the amount of edge current density and the edge safety factor[12], and the edge localized MHD mode, called the peeling-ballooning mode (PBM), can be stabilized as the stability boundaries of the infinite-$n$ ballooning mode and the kink/peeling mode become far from each other[13]. From this viewpoint, compared to the results in the high-$n$ equilibria, the stability boundary of the kink/peeling mode in the low-$n$ equilibria approaches to that of the infinite-$n$ ballooning mode, particularly at $\psi = 0.98$; in other words, the ballooning mode can become unstable easier in the low-$q$ equilibria than in the high-$q$ ones. This difference of the stability property directly affect the maximum pressure gradient at the pedestal and the $n$ number of the edge localized MHD modes, and as mentioned in the previous subsection, due to increasing the $n$ number of the unstable mode, the destabilizing effect of the sheared toroidal rotation becomes strong in the low-$q$ equilibria.

From the results in this section, we reveal that the sheared toroidal rotation destabilizes the edge localized MHD modes, and the increase of the sheared rotation reduces the achievable pressure gradient becomes smaller at the pedestal. Since this destabilizing effect becomes stronger as the $n$ number of the MHD mode increases, the sheared toroidal rotation is subject to destabilize the equilibrium with narrower second stability region of ballooning mode.

## 4. Summary

An effect of the sheared toroidal rotation has been analyzed numerically on the stability boundary of the edge localized MHD mode by using newly developed code MINERVA. We pay attention to the difference of the rotation effects on the edge MHD stability in the low-$q$ and the high-$q$ equilibria. As the result, it has been revealed that the sheared toroidal rotation has the destabilizing effect on the edge localized MHD modes, and this effect becomes stronger as the toroidal mode number of the MHD mode increases. In the numerical analyses performed in this paper, since the toroidal mode number of the edge localized MHD mode tends to be larger as the $q$ profile changes from the high-$q$ profile to the low-$q$ one, the effect of the sheared toroidal

rotation appears clearly in the low-$q$ equilibria.

In this paper, we focus on the rotation effect on the stability boundary of edge localized MHD modes. To discuss the amplitude of ELMs, it is necessary not only to investigate not only the stability boundary but also to estimate the ELM size; for example, the ELM size can be estimated with the width of the eigenfunction of the MHD mode[14]. By using the MINERVA code, the structure of the eigenfunction can be obtained, and an effect of the toroidal rotation will be discussed on as soon as possible.

Moreover, the numerical results imply that the effect of the toroidal rotation is weak on the MHD stability at the pedestal when the profile is similar to the experimental data. However, note that the edge MHD stability strongly depends on not the rotation frequency but the rotational shear near the plasma surface[5]. Also note that the measurement of the rotation profile near the plasma surface still has some ambiguities; for example, if the plasma has finite rotation frequency at the plasma surface, the edge rotational shear can multiply many times. Hence, it is important to analyze the rotation effect quantitatively and to compare with the experimental results for understanding the the dependence of the ELM frequency on the rotation effect on the edge MHD stability. These studies are necessary for revealing the physical mechanisms that link to the control/stabilizing methods of the edge localized MHD modes, which is one of the key factors to realize type-I ELM-free high performance plasmas, and we will report on the research of this issue elsewhere.

## Acknowledgments

The authors (especially N. A.) would like to thank Dr. M. Hirota for useful discussions. We also thank Dr. M. Kikuchi and Dr. H. Ninomiya for their support.

## References

[1] Oyama N, Kamada Y, Isayama A, Urano H, Koide Y, Sakamoto Y, Takechi M and Asakura N 2007 *Plasma Phys. Control. Fusion* **49** 249

[2] Oyama N, Sakamoto Y, Isayama A, Takechi M, Gohil P, Lao L L, Snyder P B, Fujita T, Ide S, Kamada Y, Miura Y, Oikawa T, Suzuki T, Takenaga H, Toi K and the JT-60 Team 2005 *Nucl. Fusion* **45** 871

[3] Snyder P B, Burrell K H, Wilson H R, Chu M S, Fenstermacher M E, Leonard A W, Moyer R A, Osborne T H, Umansky M, West W P and Xu X Q 2007 *Nucl. Fusion* **47** 961

[4] Tokuda S 1998 *J. Plasma Fusion Res.* **74** 503

[5] Aiba N, Tokuda S and Furukawa M *to be Submitted to Comput. Phys. Commun.*

[6] Tokuda S and Watanabe T 1999 *Phys. Plasmas* **6** 3012

[7] Aiba N, Tokuda S, Fujita T, Ozeki T, Chu M S, Snyder P B and Wilson H R 2007 *J. Plasma Fusion Res.* **2** 010

[8] Takeda T and Tokuda S 1991 *J. Comp. Phys.* **93** 1

[9] Frieman E and Rotenberg M 1960 *Rev. Mod. Phys.* **32** 898

[10] Bernstein I B, Frieman E A, Kruskal M D and Kulsrud R M 1958 *Proc. Roy. Soc. London* **A 244** 17

[11] Aiba N, Tokuda S, Ishizawa T and Okamoto M 2006 *Comput. Phys. Commun.* **175** 269

[12] Aiba N, Tokuda S, Takizuka T, Kurita G and Ozeki T 2007 *Nucl. Fusion* **47** 297

[13] Connor J W, Hastie R J, Wilson H R and Miller R L 1998 *Phys. Plasmas* **5** 2687

[14] Doyle E J *et al.* 2007 *Nucl. Fusion* **47** S72